Title

Lack of Sprouty 1 and 2 enhances survival of effector CD8+ T cells and yields more protective memory cells

Journal

Proceedings of the National Academy of Sciences of the United States of America, 115(38)

ISSN

0027-8424

Authors

Shehata, Hesham M
Khan, Shahzada
Chen, Elise
et al.

Publication Date

2018-09-18

DOI

10.1073/pnas.1808320115

Peer reviewed

Lack of Sprouty 1 and 2 enhances survival of effector CD8$^+$ T cells and yields more protective memory cells

Hesham M. Shehata[a], Shahzada Khan[a], Elise Chen[b,1], Patrick E. Fields[b,2], Richard A. Flavell[b,c,3], and Shomyseh Sanjabi[a,d,3]

[a]Virology and Immunology, Gladstone Institutes, San Francisco, CA 94158; [b]Department of Immunobiology, Yale University, New Haven, CT 06520; [c]Howard Hughes Medical Institute, New Haven, CT 06520; and [d]Department of Microbiology and Immunology, University of California, San Francisco, CA 94143

Contributed by Richard A. Flavell, July 16, 2018 (sent for review May 15, 2018; reviewed by Hongbo Chi and Ananda W. Goldrath)

Identifying novel pathways that promote robust function and longevity of cytotoxic T cells has promising potential for immunotherapeutic strategies to combat cancer and chronic infections. We show that sprouty 1 and 2 (Spry1/2) molecules regulate the survival and function of memory CD8$^+$ T cells. Spry1/2 double-knockout (DKO) ovalbumin (OVA)-specific CD8$^+$ T cells (OT-I cells) mounted more vigorous autoimmune diabetes than WT OT-I cells when transferred to mice expressing OVA in their pancreatic β-islets. To determine the consequence of Spry1/2 deletion on effector and memory CD8$^+$ T cell development and function, we used systemic infection with lymphocytic choriomeningitis virus (LCMV) Armstrong. Spry1/2 DKO LCMV gp33-specific P14 CD8$^+$ T cells survive contraction better than WT cells and generate significantly more polyfunctional memory T cells. The larger number of Spry1/2 DKO memory T cells displayed enhanced infiltration into infected tissue, demonstrating that absence of Spry1/2 can result in increased recall capacity. Upon adoptive transfer into naive hosts, Spry1/2 DKO memory T cells controlled *Listeria monocytogenes* infection better than WT cells. The enhanced formation of more functional Spry1/2 DKO memory T cells was associated with significantly reduced mTORC1 activity and glucose uptake. Reduced p-AKT, p-FoxO1/3a, and T-bet expression was also consistent with enhanced survival and memory accrual. Collectively, loss of Spry1/2 enhances the survival of effector CD8$^+$ T cells and results in the formation of more protective memory cells. Deleting Spry1/2 in antigen-specific CD8$^+$ T cells may have therapeutic potential for enhancing the survival and functionality of effector and memory CD8$^+$ T cells in vivo.

CD8 T cells | memory | metabolism | survival | polyfunctional

Immunotherapeutic strategies that enhance cytotoxic T cell functionality and longevity have the potential to combat cancer and chronic viral infections (1–3). The defining hallmarks of long-lived memory CD8$^+$ T cells are their increased numbers, broader anatomical distribution, and enhanced function compared with naive cells (4–10). Pharmacologic interventions or genetic modifications that result in enhanced memory CD8$^+$ T cells lead to more robust recall responses and better protection against antigen reexposure (5–7, 11–17). Memory development relies on the integration of signals arising from T cell receptor (TCR) signaling strength, cytokines, metabolic reprograming, and modular expression of lineage-specific transcription factors (18, 19).

To become activated, T cells engage via their TCR with MHC complexes that present their cognate peptide. TCR stimulation also results in inhibitory signals that restrain excessive T cell activation to prevent autoimmunity and maintain homeostasis. Such inhibitory mechanisms may also dampen desirable immune responses during vaccination or against chronic pathogens and tumors (20). While targeting inhibitory mechanisms such as CTLA-4 and PD-1 have been well studied (21–23), less is known about the intracellular inhibitory molecules that are up-regulated by TCR signaling (3). Efforts to find novel negative regulators of T cell signaling identified Sprouty (Spry) molecules (24). Spry was initially discovered in a genetic screen as an inhibitor of *Drosophila* fibroblast growth factor receptor signaling during trachea development (25). Four mammalian homologs (Spry1–4) have been identified, and their inhibitory effects are mainly ascribed to their ability to inhibit Ras–MAPK signaling (26, 27).

Upon TCR engagement, Spry1 is highly induced (24), translocates to the immune synapse, and interacts with and inhibits the activation of linker for activated T cells (LAT) and phospholipase C-γ (PLC-γ) (28, 29). Spry2 is present in naive T cells, is further induced upon TCR stimulation (24), and also inhibits PLC-γ (29). By inhibiting these key adaptors downstream of TCR signaling, Spry 1 and Spry 2 inhibit activation of MAPK signaling and NFκB, NFAT, and AP-1 transcription factors and limit T cell activation and proliferation and IL-2 production in cell lines and primary T cells in vitro (24, 28, 29). Conditional deletion of Spry1 in mouse CD4$^+$ and CD8$^+$ T cells did not influence their thymic development but enhanced IL-2 and IFN-γ production and boosted their capacity to clear EL4 lymphoma cells and lung B16 melanoma tumor nodules in vivo (30). Additionally, Spry2 mRNA and protein levels are up-regulated in HIV-specific CD8$^+$ T cells and contribute to the exhaustion of these cells (31). Collectively, these studies suggest that Spry 1 and Spry 2 molecules may act as negative regulators of TCR signaling.

In this study, we examined the role of Spry 1 together with Spry 2 deficiency in the formation and function of effector and

Significance

Sprouty (Spry) molecules are known regulators of the Erk signaling pathway. We determined how the absence of Spry 1 and Spry 2 affects the formation and function of effector and memory CD8$^+$ T cells. We found that absence of Spry1/2 enhances the survival of effector CD8$^+$ T cells and results in the formation of more polyfunctional memory cells. As increased numbers of memory CD8$^+$ T cells strongly correlate with enhanced protection against tumors and pathogenic infections, our findings identify the *Spry1* and *Spry2* loci as attractive targets for increasing the number, survival, and function of antigen-specific memory CD8$^+$ T cells. This may provide an opportunity for better future engineering of T cells against tumors and chronic viral infections.

Author contributions: H.M.S. and S.S. designed research; H.M.S. and S.K. performed research; E.C., P.E.F., and R.A.F. contributed new reagents/analytic tools; H.M.S. and S.S. analyzed data; and H.M.S. and S.S. wrote the paper.

Reviewers: H.C., St. Jude Children's Research Hospital; and A.W.G., University of California, San Diego.

The authors declare no conflict of interest.

See Commentary on page 9339.

[1]Present address: PRA Health Sciences, Lenexa, KS, 66219.

[2]Present address: Department of Pathology and Laboratory Medicine, University of Kansas Medical Center, Kansas City, KS 66160.

[3]To whom correspondence may be addressed. Email: richard.flavell@yale.edu or shomyseh.sanjabi@gladstone.ucsf.edu.

This article contains supporting information online at www.pnas.org/lookup/suppl/doi:10.1073/pnas.1808320115/-/DCSupplemental.

Published online August 20, 2018.

memory CD8$^+$ T cells. Spry1/2 double-knockout (DKO) T cells formed larger numbers of functional memory CD8$^+$ T cells, which was associated with significantly reduced mTORC1 activity and glucose uptake. As the increased number of memory CD8$^+$ T cells strongly correlates with enhanced protection against tumors and pathogenic infections (5, 7, 11–16), our findings suggest that targeting both Spry1/2 molecules may be beneficial for boosting the number of antigen-specific memory CD8$^+$ T cells in vivo.

Results

Spry1/2 Are Induced upon TCR Stimulation. To determine which Spry members are expressed in CD8$^+$ T cells, we measured relative steady-state mRNA expression of Spry1–4 in mouse naive CD8$^+$ T cells. Similar to published results (24, 30), we detected higher mRNA expression of Spry2 and Spry4 than of Spry1 and Spry3 (*SI Appendix*, Fig. S1*A*). Upon TCR stimulation using anti-CD3 and anti-CD28 mAbs, only Spry1 and Spry2 mRNA were induced (*SI Appendix*, Fig. S1*B*). Furthermore, the steady-state expression of Spry1 and Spry2 was three- to fourfold higher in central memory cells than in naive CD8$^+$ T cells (*SI Appendix*, Fig. S1*B*, 0 time points), suggesting that Spry1/2 may be important for the development and/or function of memory T cells. High induction of Spry1 (50- to 80-fold) and moderate induction of Spry2 (1.5- to threefold) in all T cell subsets after TCR stimulation is consistent with their proposed roles as regulators of TCR signaling (24, 28, 29). However, we reasoned that the unaltered expression of Spry3–4 during T cell maturation and upon TCR stimulation suggests that they may not play a role in modulating TCR signaling.

Spry1 and Spry2 share many structural and functional features (32–34). To eliminate any compensatory effects of Spry1 in the absence of Spry2 (and vice versa), we generated mice that are floxed for *Spry1* and *Spry2* genes (*SI Appendix*, Fig. S2 *A* and *B*) and crossed them to each other and to CD8-Cre mice (Cre being expressed in peripheral CD8$^+$ T cells) (35) to generate DKO animals. The DKO animals crossed to OTI-I or P14 TCR transgenic T cell mice on a *Rag1*$^{-/-}$ background maintained a naive phenotype under steady-state conditions (*SI Appendix*, Fig. S2*C*) and failed to express Spry1/2 mRNA upon TCR stimulation with anti-CD3 and anti-CD28 (*SI Appendix*, Fig. S2*D*). Thus, we have created a system in which we can unambiguously determine the consequence of the absence of both Spry1 and Spry2 in antigen-specific CD8 T cells in response to their cognate antigen in vivo.

Spry1/2 DKO CD8$^+$ T Cells Accelerate the Onset of Type I Diabetes in Rat Insulin Promoter–Membrane-Bound Ovalbumin Mice. To determine if the absence of Spry1/2 enhances cytotoxicity, we used rat insulin promoter (RIP)–membrane-bound ovalbumin (mOVA) transgenic mice that express mOVA in the pancreas under the control of the RIP (36). In this system, adoptive transfer of 5×10^6 naive OT-I T cells is sufficient to cause diabetes in 100% of the mice within 4 wk (37). We adoptively transferred 1×10^6 OT-I DKO or OT-I WT T cells into either RIP-mOVA transgenic mice or WT mice (Fig. 1*A*). The onset of diabetes was determined by measuring blood and urine glucose over a 3-wk period after OT-I T cell transfer. At 2 wk, 12.5% of RIP-mOVA animals that received DKO cells remained nondiabetic compared 67% of animals that received WT cells (Fig. 1*B*). By 3 wk, all the RIP-mOVA animals that received DKO OT-I T cells became diabetic, compared with only a fraction of WT OT-I T cell recipients (Fig. 1*B*). In contrast, neither WT nor DKO OT-I T cells induced hyperglycemia in WT recipients (Fig. 1*B*). These data suggest that in the absence of Spry1/2, naive CD8$^+$ T cells gain the ability to induce hyperglycemia more quickly in the RIP-mOVA mouse model of type I diabetes.

Spry1/2 Limit Early Effector Differentiation During Acute Viral Infection. To determine if Spry1/2 limit T cell activation, proliferation, and effector differentiation under virally induced inflammatory conditions, we coadoptively transferred carboxyfluorescein succinimidyl ester (CFSE)-labeled DKO P14 (CD45.1.1) and WT P14 (CD45.1.2) T cells at a 1:1 ratio into CD45.2.2 WT recipients (Fig. 2*A*). These chimeric animals were infected with lymphocytic choriomeningitis virus (LCMV) Armstrong (LCMV$_{ARM}$), and T cell activation and CFSE dilution of DKO and WT P14 T cells in each WT host was measured 3 d postinfection (d.p.i.). In the peritoneal-draining mediastinal lymph nodes (Med LNs) (38), WT and DKO P14 T cells up-regulated CD69 and CD25 and similarly diluted CFSE upon priming (*SI Appendix*, Fig. S3 *A–D*) in the same host. However, a larger fraction of DKO P14 T cells in the spleen expressed CD43 by 3 d.p.i., as measured by anti-CD43 mAb staining that recognizes CD43 carrying core 2 O-glycan branches (Fig. 2*B*), which are critical for the migration of effector T cells into tissues (39). Consistent with this, at day 6 postinfection (p.i.), a higher fraction of DKO cells expressed KLRG-1, and they expressed it at a higher mean fluorescent intensity (MFI) than the WT cells (Fig. 2*C*). Our data show that the absence of Spry1/2 accelerates the expression of CD43 and KLRG-1 on effector CD8$^+$ T cells under virally induced inflammatory conditions, suggesting that absence of Spry1/2 molecules leads to faster effector CD8$^+$ T cell differentiation.

Absence of Spry1/2 Limits CD8$^+$ T Cell Contraction and Promotes the Formation of a Larger Quantity of Memory CD8$^+$ T Cells. To determine the role of Spry1/2 in regulating clonal expansion and contraction of T cells, we compared the number of DKO and WT P14 T cells during early activation (day 3), clonal expansion (day 6), peak (day 8), contraction (day 13), and memory phase (day 50). We generated chimeric mice containing coadoptively transferred congenically marked WT and DKO P14 T cells followed by LCMV$_{ARM}$ infection

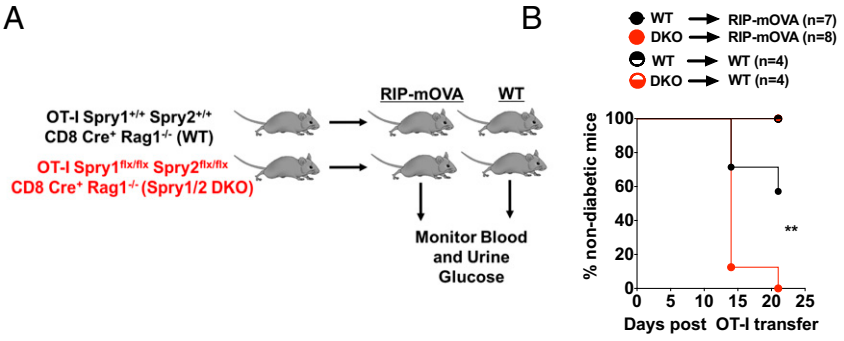

Fig. 1. Spry1/2 DKO CD8$^+$ T cells induce faster onset of type I diabetes in RIP-mOVA mice. (*A*) WT or Spry1/2 DKO OT-I T cells (1×10^6) were adoptively transferred into either WT or RIP-mOVA mice. (*B*) Blood and urine glucose levels of recipients were measured consecutively, and the compiled disease incidence after adoptive OT-I T cell transfer was determined and reported as the percentage of nondiabetic mice (<250 mg/dL). $^{**}P < 0.009$ using a log-rank test. Data are pooled from two independent experiments.

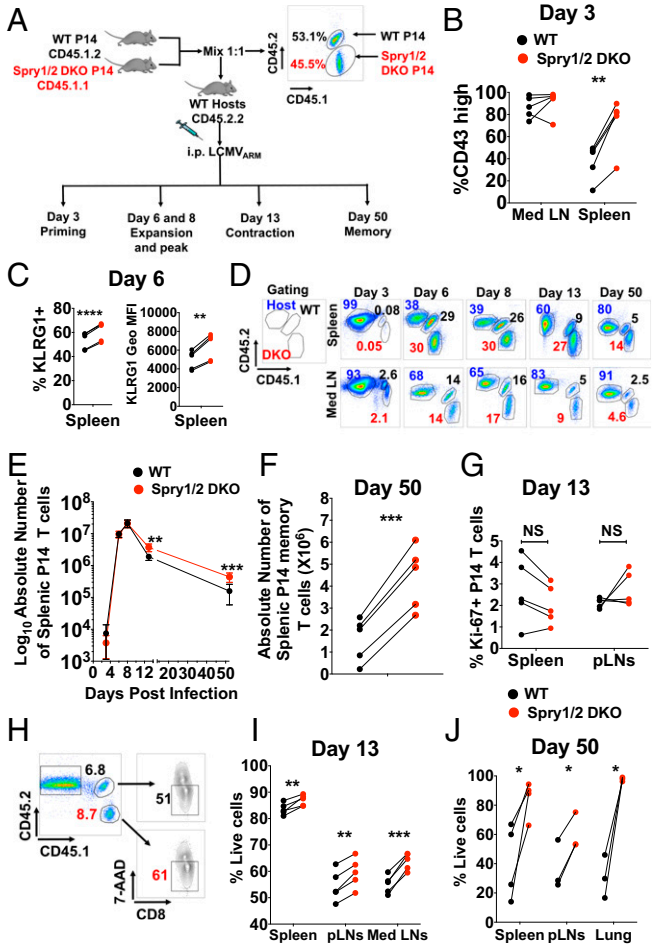

Fig. 2. The absence of Spry1/2 enhances early differentiation and the survival of effector and memory CD8$^+$ T cells. (*A*) WT and Spry1/2 DKO P14 T cells were cotransferred at 1:1 ratio into WT hosts. Chimeric mice were infected with 2×10^5 pfu LCMV$_{ARM}$, and Med LN, spleens, and pLNs were harvested. (*B–J*) Two hundred fifty thousand each (*B*) or 20,000 each (*C–J*) of WT (black) and Spry1/2 DKO (red) P14 T cells were cotransferred into WT hosts. (*B*) The proportion of CD43^{hi} (1B11) cells among the P14 T cells 3 d.p.i. (*C*) The frequency (*Left*) and geometric MFI (Geo MFI) (*Right*) of KLRG1 in splenic P14 T cells. (*D*) The frequency of transferred WT and Spry1/2 DKO P14 T cells within total CD8$^+$ T cells in the spleen (*Upper*) and Med LN (*Lower*). (*E*) Log$_{10}$ absolute number of P14 T cells from each genotype in the spleen over the course of infection. (*F*) The absolute number of memory P14 T cells in the spleen at 50 d after LCMV$_{ARM}$ infection. (*G*) The percentage of Ki-67$^+$ effector P14 T cells during the contraction phase. NS, not significant. (*H–J*) Spry1/2 DKO and WT effector cell (*H* and *I*) and memory CD8$^+$ T cell (*J*) survival was determined ex vivo by quantifying the percent of 7ADD-negative cells after 24 h in culture. Data are representative of two independent experiments with $n = 4$–5 mice per group. Each point represents one individual mouse. The *P* values represent the difference between WT and DKO P14 T cells (paired *t* test): $*P < 0.05$, $**P < 0.009$, and $***P < 0.0005$.

(Fig. 2*A*). Frequencies and absolute numbers of each expanded population were enumerated in the spleen and the Med LNs (Fig. 2 *D* and *E*). While the absence of Spry1/2 did not alter the frequencies or numbers of P14 T cells during clonal expansion or alter the peak of the response, significantly higher numbers of DKO effector CD8$^+$ T cells remained during contraction (Fig. 2*E*), and more memory cells were formed (Fig. 2 *E* and *F*).

Reduced Contraction of Effector T Cells and the Accrual of Memory Cells in the Absence of Spry1/2 Are Associated with Enhanced Survival. The majority of effector T cells die by apoptosis during contraction after viral clearance (40, 41). Lack of Spry1/2 may limit the contraction of effector T cells by enhancing either their proliferation or their survival. As a measure of proliferative potential, we measured the expression of the nuclear proliferation antigen Ki-67 during contraction. No significant difference was observed in the proportion of the Ki-67$^+$ cells between paired DKO and WT P14 T cells (Fig. 2*G*). To test whether the higher number of DKO effector and memory T cells was due to enhanced survival, we cultured splenocytes containing DKO and WT P14 effector or memory T cells from chimeric mice ex vivo for 24 h and measured the percentage of live cells. In the absence of Spry1/2, effector T cells (Fig. 2 *H* and *I*) and memory T cells (Fig. 2*J*) had a survival advantage compared with WT T cells. Thus, in the absence of Spry1/2, more effector CD8$^+$ T cells survive the contraction phase and continue to differentiate to form a larger number of memory cells.

Absence of Spry1/2 Promotes the Development of a Larger Number of Memory T Cell Precursors. After clonal expansion, a heterogeneous population of effector T cells is generated. The most terminally differentiated effectors, known as "terminal effector" (TE) cells, express high amounts of KLRG1 and low amounts of IL-7Rα (CD127) (42–44). Most of these TE cells die by apoptosis during contraction, but some persist as circulating memory T cells (42–46). The remaining smaller fraction of effector T cells that are memory precursor (MP) cells survive the contraction and form the long-lived pool of memory T cells. MP cells are among the CD127^{hi} KLRG1^{low} population, which is long-lived and has multipotent characteristics that allow them to self-renew and regenerate new clonal bursts of effectors upon rechallenge (43, 44).

To determine whether the absence of Spry1/2 alters the commitment of effector T cells to either TE or MP cells, we measured the proportions and absolute numbers of these effector subsets as well as the double-positive (CD127^{hi} KLRG1^{hi}) (DP) and early effector (CD127^{low} KLRG1^{low}) (EE) T cells (43, 44). At contraction, the absolute numbers of all effector subsets were increased, and the DP and MP fractions, in particular, were significantly increased in the absence of Spry1/2 (Fig. 3*A*). When comparing the ratios of the various WT and DKO effector T cells, the DKO population contained a slightly higher fraction of MP cells, which was accompanied by a slight reduction in the proportion of TE cells during contraction (Fig. 3*B*).

We also examined whether the absence of Spry1/2 alters the ability of effector T cells to produce effector molecules. WT and DKO P14 T cells isolated 8 and 13 d after LCMV$_{ARM}$ infection were stimulated ex vivo with gp33 peptide (Fig. 3 *C* and *D*). At day 8 p.i., a similar fraction and number of WT and DKO P14 T cells produced IFN-γ, TNF-α, and CD107a (Fig. 3*C*). However, when we enumerated the number of P14 T cells producing different combinations of effector molecules at day 13 p.i., we observed a marked increase in the number of polyfunctional DKO T cells compared with their WT counterparts in the same host (Fig. 3*D*). Thus, these data suggest that the absence of Spry1/2 does not impair cytolytic function or cytokine production and that fully functional effectors can better survive the contraction phase.

To determine if the absence of Spry1/2 alters the in vivo functionality of effector T cells to control viral infection, we used our LCMV intrarectal (i.rec.) infection model (47). In the i.rec. model CD8$^+$ T cell priming is delayed by about 48 h compared with i.p. infection (48). We delivered LCMV$_{ARM}$ i.rec. to B6 chimeric animals that were generated after independent transfer of either WT or DKO P14 T cells and measured colonic viral clearance at day 12 p.i. (*SI Appendix*, Fig. S4). Consistent with our findings that WT and DKO effector T cells produce similar amounts of effector molecules ex vivo, these results demonstrate that WT and DKO effector T cells have similar functionality in vivo at a time when similar numbers of effector T cells are present in each host.

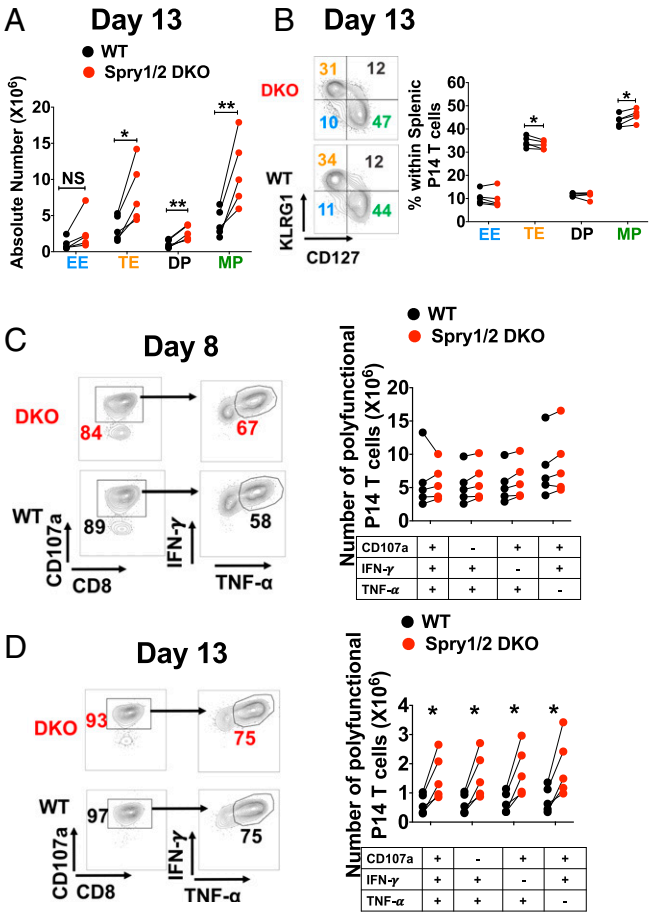

Fig. 3. The absence of Spry1/2 in T cells promotes the formation of functional effectors that are skewed toward memory precursors. (*A* and *B*) The absolute numbers (*A*) and frequencies (*B*) of Spry1/2 DKO and WT P14 effector T cell subsets during contraction at day 13 p.i. (*C* and *D*) Splenocytes isolated on day 8 (*C*) and day 13 (*D*) were stimulated with gp33 peptide ex vivo, and effector cytokines and degranulation from P14 T cells were measured. (*Left*) Gating strategy for cytokine production analyses. (*Right*) The absolute numbers of P14 T cells producing different combinations of cytokines and CD107a (Lamp-1). Data are representative of two independent experiments with $n = 4$–5 mice per group. Each point represents one individual mouse. The *P* values in *A*–*D* represent the difference between WT and DKO P14 T cells using a paired *t* test: $*P < 0.05$ and $**P < 0.009$. NS, not significant.

Enhanced Number of Polyfunctional Memory CD8$^+$ T Cells in the Absence of Spry1/2 Results in Faster Recall Capacity. A principle characteristic of immunological memory is the capacity to mount accelerated recall responses with higher magnitude upon antigen reexposure. To determine if the absence of Spry1/2 alters memory recall responses, B6 chimeric memory animals containing both WT and DKO P14 memory T cells were rechallenged with $LCMV_{ARM}$ intranasally (i.n.), and the recall responses of WT and DKO P14 T cells were measured 2 d later. DKO P14 T cells displayed enhanced recall responses in the lungs of rechallenged animals (Fig. 4*A*). We reasoned that the more robust recall response may be due to the larger number of DKO memory T cells that are generated in the lung upon systemic infection. To determine whether the absence of Spry1/2 enhances the capacity of memory CD8$^+$ T cells to migrate into infected tissues, we purified DKO and WT memory P14 T cells, mixed them at a 1:1 ratio, and retransferred them into naive hosts that were subsequently infected i.n. with $LCMV_{ARM}$. When memory T cells were present at a 1:1 ratio, the DKO memory T cells showed no significant enhancement in their ability to migrate into the infected lungs (Fig. 4*B*). These data suggest that DKO memory T cells have enhanced recall capacity due to the presence of larger numbers of memory cells before rechallenge.

To determine if the absence of Spry1/2 enhances memory CD8$^+$ T cell polyfunctionality in response to their cognate antigen, splenocytes isolated on day 50 were stimulated with gp33 peptide ex vivo, and effector cytokines and granzyme B (GZB) production from P14 T cells were measured. While the fraction of memory T cells producing these cytokines was generally unaltered, a

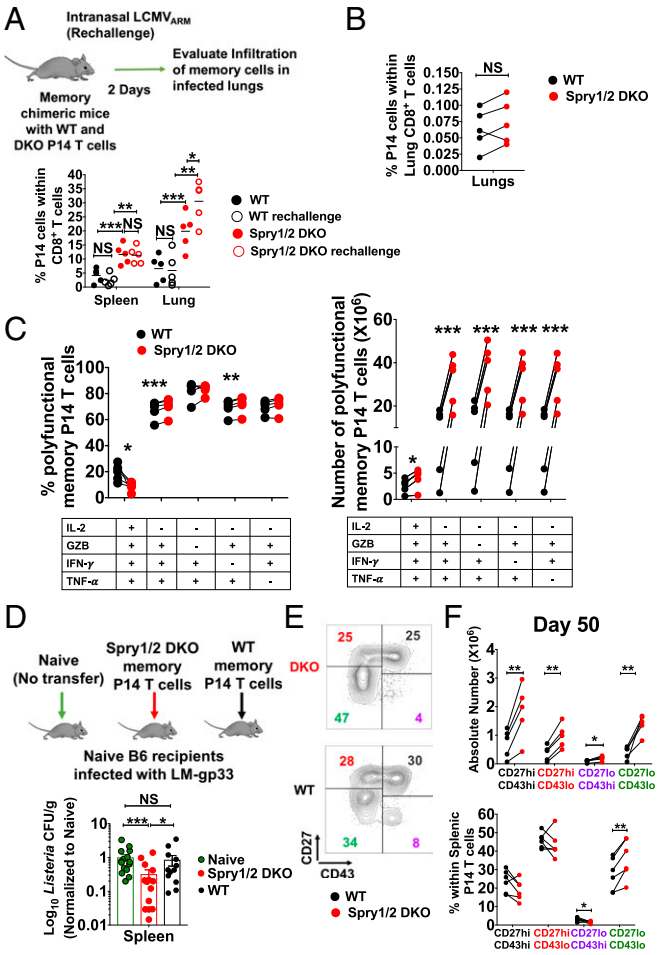

Fig. 4. The absence of Spry1/2 promotes the formation of larger numbers of polyfunctional memory CD8$^+$ T cells with superior protective capacity. (*A*) Chimeric animals generated by transferring WT and DKO P14 T cells were immunized i.p. with 2×10^5 pfu $LCMV_{ARM}$ and 50 d later were rechallenged i.n. with 8×10^5 pfu of $LCMV_{ARM}$. Recall responses of WT and DKO P14 T cells were measured 2 d later in the spleen and lung. (*B*) Memory P14 T cells from WT and DKO chimeric animals were purified by flow cytometry, mixed at a 1:1 ratio, and adoptively transferred into naive mice. Chimeric mice were then challenged i.n. with 8×10^5 pfu of $LCMV_{ARM}$, and the proportion of P14 T cells infiltrating the lungs was measured. (*C*) The frequency (*Left*) and number (*Right*) of polyfunctional memory P14 T cells after ex vivo stimulation with gp33 peptide. (*D*) WT and Spry1/2 DKO memory P14 T cells were purified from the spleen and pLNs of donor chimeric animals by flow cytometry and were retransferred into naive hosts that were then challenged with recombinant *L. monocytogenes* expressing LCMV gp33 (LM-gp33). (*E* and *F*) The absolute number (*E*) and fraction of each memory T cell subset (*F*) was measured based on differential surface expression of CD27 and CD43 on memory P14 T cells in the spleen at day 50 after $LCMV_{ARM}$ infection. Data are representative of two independent experiments. Each point represents one individual mouse. The *P* values represent the difference between WT and DKO P14 T cells (paired *t* test): $*P < 0.05$, $**P < 0.009$, and $***P < 0.0005$. NS, not significant.

significantly larger number of polyfunctional DKO P14 memory T cells was present in these chimeric animals (Fig. 4*C*). To test the functional sensitivity to low-dose peptide–MHC ligand, we stimulated the cells with a titration of gp33 peptide and found that DKO and WT memory P14 T cells have a similar dose response (*SI Appendix*, Fig. S5 *A–C*). Taken together, our data suggest that in the absence of Spry1/2 a larger number of polyfunctional memory cells is generated.

Memory CD8$^+$ T Cells Display Better Protective Capacity in the Absence of Spry1/2. To determine whether bona fide memory T cells from a DKO origin have an enhanced protective capacity on a per-cell basis in vivo, WT and DKO memory P14 T cells were purified by flow cytometry from donor chimeric animals. Thirty thousand cells of each population were retransferred into uninfected hosts that were then challenged with recombinant *Listeria monocytogenes* expressing gp33 (LM-gp33). At 2 d.p.i. the recipients of DKO memory P14 T cells had significantly lower bacterial burden (Fig. 4*D*). These results highlight that deleting Spry1/2 can enhance the protective functionality of memory CD8$^+$ T cells.

The memory CD8$^+$ T cell pool comprises distinct subsets with unique characteristics, including tissue trafficking, effector function, and recall responses. Memory T cells characterized based on CD27 and CD43 expression differ in recall and protective responses (45, 49). The CD27^{hi} CD43^{lo} memory cells are maintained long term and demonstrate superior cellular expansion upon antigen reencounter (49). In contrast, CD27^{lo} CD43^{lo} memory cells do not expand as much but display superior protective immunity against *Listeria* and vaccinia virus infection (45). We sought to determine if the enhanced protective functionality against *Listeria* in the absence of Spry1/2 was associated with the development of larger numbers of CD27^{lo} CD43^{lo} memory T cells. Absolute numbers of all memory subsets were increased in the absence of Spry1/2 (Fig. 4 *E* and *F*). However, we did indeed identify a significantly higher proportion of CD27^{lo} CD43^{lo} T cells among DKO cells than in WT P14 T cells (Fig. 4*F*), which correlated with enhanced protection against *Listeria* (45). These data suggest that the absence of Spry1/2 results in altered memory subsets, which may provide a protective advantage under certain infection conditions.

Absence of Spry1/2 Is Associated with Reduced Activity of the mTORC1–AKT–FoxO1 Signaling Axis. To address how DKO CD8$^+$ T cells form more memory cells, we reasoned that Spry1/2 may regulate the activity of the metabolic checkpoint kinase, mechanistic target of rapamycin (mTOR), which is essential for sustaining the activation and survival of effector and memory CD8$^+$ T cells. mTOR coordinates effector and memory CD8$^+$ T cell generation in part by controlling both metabolic and transcriptional reprogramming through the mTORC1–mTORC2–AKT–FoxO1 signaling axis, which controls the downstream master transcription factors T-bet, Eomesodermin (Eomes), and Tcf-1 (14, 16, 50–53). These transcription factors, in turn, are critical in orchestrating the development of memory CD8$^+$ T cells (14, 43, 54–56).

We measured the phosphorylation of S6, which is a direct target of mTORC1 (11, 57), in coadoptively transferred WT and DKO P14 CD8$^+$ T cells during the priming, effector, and contraction phases. While mTORC1 activity was similar in WT and DKO P14 T cells during priming at 3 d.p.i. (Fig. 5*A*), it was significantly reduced in DKO P14 T cells during the effector and contraction phases when measured directly ex vivo (Fig. 5*A*). To further confirm these results, we restimulated effector P14 T cells with gp33 peptide and measured the phosphorylation of S6 and 4-EBP1 during contraction (Fig. 5*B*); the lower phosphorylation of these molecules in DKO P14 T cells was consistent with the ex vivo data (Fig. 5*A*). Furthermore, we observed a significant reduction in glucose uptake in DKO compared with

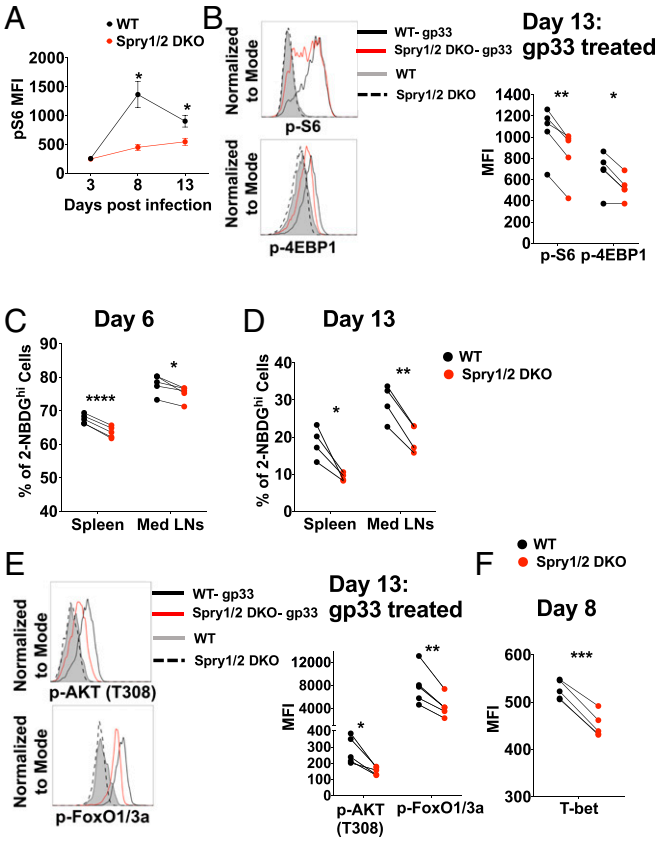

Fig. 5. The absence of Spry1/2 is associated with reduced activity of the mTORC1–AKT–FoxO1/3a signaling axis. mTORC1 activity was evaluated in chimeric mice harboring both WT and DKO P14 T cells after infection with 2×10^5 pfu LCMV$_{ARM}$. (*A*) p-S6 intensity was measured directly ex vivo as a marker of mTORC1 activity in WT and DKO P14 T cells isolated from Med LNs of chimeric mice at 3, 8, and 13 d.p.i. (*B*) Representative histograms and MFI of WT (solid black line) and DKO (red line) P14 effector T cells from day 13 after LCMV$_{ARM}$ infection after ex vivo gp33 stimulation. Splenocytes were harvested and rested for 2–4 h, followed by restimulation with gp33 peptide for 60 min. p-S6 and p-4EBP1 were measured by phospho-flow. The shaded histogram and dotted histogram are unstimulated WT P14 and DKO P14 effector T cells, respectively. (*C* and *D*) Extracellular glucose uptake was measured in the spleen by ex vivo uptake of 2-NBDG by P14 T cells at 6 (*C*) and 13 (*D*) d.p.i. (*E*) Representative histograms and MFI of WT (solid black line) and DKO (red line) P14 effector T cells from day 13 after LCMV$_{ARM}$ infection after ex vivo gp33 stimulation. Splenocytes were harvested and rested for 2–4 h, followed by restimulation with gp33 peptide for 60 min, and p-AKT(T308) and p-FoxO1/3a were measured by phospho-flow. The shaded histogram and dotted histogram show unstimulated WT P14 and DKO P14 effector T cells, respectively, from LCMV$_{ARM}$-infected mice. (*F*) The expression level of T-bet in WT and Spry1/2 DKO effector P14 T cells at the peak of the response. The y axes of histogram overlays were normalized to mode. Data are representative of two independent experiments with $n = 4$–5 mice per group. Each point represents one individual mouse. The *P* values represent the difference between WT and DKO P14 T cells (paired *t* test): $*P < 0.05$, $**P < 0.009$, and $***P < 0.0005$.

WT P14 T cells (Fig. 5 *C* and *D*). Lower mTORC1 activity and glucose uptake are both commensurate with enhanced memory development (11, 12, 14–16, 50–52, 57).

The mTORC1–mTORC2–Akt–FoxO1 signaling axis plays a critical role in CD8$^+$ T cell memory development via specific transcriptional reprogramming (14, 16, 50–53). Nuclear FoxO1 directly regulates the expression of T-bet and Eomes, and loss of FoxO1 impairs memory development and recall responses (13, 14, 50, 51). In addition to other posttranslational modifications, FoxO1 activity is primarily governed by PI3K-Akt and

mTORC1/mTORC2-dependent Akt-mediated phosphorylation, which leads to its nuclear export and loss of transcriptional activity. In particular, the phosphorylation of FoxO1 is controlled by the phosphorylation of Akt at T308 (downstream of PI3K) (58) and S473 (downstream of mTORC2) (59). Phosphorylation of both Akt (T308) and FoxO1/3a was significantly reduced in DKO effector P14 T cells examined after gp33 restimulation on day 13 (Fig. 5*E*), suggesting enhanced nuclear localization of FoxO1/3a. In line with enhanced nuclear FoxO1/3a, T-bet expression was also significantly reduced in DKO T cells (Fig. 5*F*). Lower mTORC1 activity, reduced glucose uptake, reduced PI3K-mediated activation of Akt, and enhanced nuclear FoxO1/3a are all commensurate with enhanced development of memory $CD8^+$ T cells (11, 12, 14–16, 50–52, 57). Our data show that $CD8^+$ T cell memory formation is enhanced in the absence of Spry1/2 and that this is mediated, at least in part, by altered activity of the mTORC1–AKT–FoxO1 signaling axis.

Discussion

In this study, we report that the absence of Spry1/2 in $CD8^+$ T cells enhances the survival of effector T cells and results in the formation of more memory T cells, leading to enhanced protective capacity. We demonstrate that the larger number of memory T cells at the time of rechallenge allows them to mount robust recall responses more readily. Indeed, generation of larger numbers of memory $CD8^+$ T cells is associated with enhanced host protection upon a second encounter with the same antigen (5–7, 11–16). In addition, when functional responses were compared on a per cell basis, DKO memory T cells conferred enhanced protection against *Listeria* infection. Our findings identify the *Spry1/2* loci as attractive genetic targets for increasing the number and function of antigen-specific memory $CD8^+$ T cells, which may provide an opportunity for the future development of better immunotherapies against tumors and chronic viral infections (2, 60).

We also found that in the absence of Spry1/2 OT-I T cells induced a faster onset of autoimmune diabetes when transferred into RIP-mOVA mice. These data suggest that the Spry1/2 DKO naive $CD8^+$ T cells are readily activated and induce faster hyperglycemia in RIP-mOVA mice than their WT counterparts.

In the absence of Spry1/2, the larger number of effector $CD8^+$ T cells during contraction and subsequently in the memory phase was associated with enhanced survival. Our finding supports a role for reduced mTORC1 activity, lower glucose uptake, and enhanced nuclear FoxO1/3a in augmenting memory T cell development and survival in the absence of Spry1/2. High mTORC1 activity in effector T cells is closely coupled to high glycolytic capacity, while memory $CD8^+$ T cells have decreased mTORC1 activity and decreased glycolytic capacity (15, 16, 57, 61–64). Enhanced nuclear FoxO1 is consistent with enhanced survival. However, the exact antiapoptotic pathway that contributes to enhanced survival of $CD8^+$ T cells that lack Spry1/2 molecules remains to be determined.

TCR signaling begins with phosphorylation of the ζ-chain of the CD3 complex coupled to the α- and β-chains of TCR. Subsequently, the tyrosine kinase ZAP70 binds to the phosphorylated ζ-chain and becomes activated (65). Activated ZAP70 phosphorylates LAT, which recruits Grb2, Grb2-related adaptor protein 2 (GADS), Src homology 2 domain-containing leukocyte protein of 76kDa (SLP76), and PLC-γ1 (66). PLC-γ1 in turn hydrolyzes PIP2 into inositol 3,4,5-triphosphate (IP3) and diacylglycerol (DAG) (67). IP3 activates the calcium–NFAT pathway, while DAG activates the PKCθ–NF-κB and Ras–MAPK pathways (68). In vitro biochemical studies suggest that Spry1/2 are recruited to the immune synapse upon TCR engagement and subsequently interact and inhibit the phosphorylation and activation of adaptors, including LAT and PLC-γ (24, 28, 29). Through these interactions Spry1/2 may inhibit the MAPK–ERK, NFκB, NFAT, and AP-1 cascades. However, in this study, we did not observe biologically significant differences in WT and DKO effector P14 T cell expansion, cytokine production, or in vivo function. While the up-regulation of the early activation markers CD69 and CD25 was similar in DKO and WT P14 T cells at the time of priming, the DKO effector T cells did up-regulate CD43 and KLRG1 faster than WT T cells. Thus, our in vivo data suggest that in the absence of Spry1/2 $CD8^+$ T cell activation likely occurs normally, but effector differentiation may occur faster. It remains to be determined exactly how the combination of Spry1/2 molecules functions to regulate T cell differentiation in vivo.

In this study, we also identified an intriguing link between Spry1/2 molecules and effector T cell metabolism. How the absence of Spry1/2 leads to reduced mTORC1 and AKT activation is unknown, but given the previously described biochemical interaction of Spry1/2 with TCR signaling adaptors (24, 28, 29), a number of potential mechanisms emerge. In the absence of Spry1/2, stronger TCR stimulation may result in the induction of negative feedback pathways that inhibit mTORC1. Strong TCR signaling activates AMP kinase (AMPK) through the adaptors LAT and SLP-76 via PLC-γ–mediated release of Ca^{2+} (69). Activation of AMPK inhibits mTORC1 activity (70–72). Thus, augmented TCR signaling in the absence of Spry1/2 could lead to higher AMPK activity that inhibits mTORC1 and glucose uptake, which may contribute to the enhanced generation and functionality of memory $CD8^+$ T cells. Alternatively, Spry1/2 can interact with and sequester Cbl-b/c-Cbl (28, 73–75), which are negative inhibitors of PI3K activation (76). As PI3K stimulates both mTORC1 and AKT, lower P13K action due to higher Cbl-b/c-Cbl activity may also cause lower mTORC1 function. PI3K activation results in AKT phosphorylation at T308, which we found to be lower in DKO P14 T cells, suggesting there is indeed lower PI3K activity and potentially enhanced Cbl-b/c-Cbl activity in the absence of Spry1/2. FoxO1 phosphorylation is regulated by phosphorylation of Akt at T308 downstream of PI3K (58) and at S473 downstream of mTORC2 (59). As we observe reduced phosphorylation of FoxO1, we would predict lower levels of pAktS473 as well. However, future studies are needed to further elucidate the precise signaling cascade that leads to lower mTORC1 activity and to determine if mTORC2 activity is also lower in the absence of Spry1/2 molecules.

The identification of Spry1/2 as intracellular inhibitors that function to limit T cell proliferation, survival, and memory formation would make them attractive targets for enhancing tumor immunotherapy. Indeed, transiently targeting inhibitors that restrain T cell activation, such as CTLA-4 and PD-1, have produced impressive antitumor results in the clinic (77–81). However, targeting these checkpoints is also fraught with immune-related toxicities (2, 20, 82–85). Therefore, identifying novel candidate immunoregulatory checkpoints that can be targeted either independently or in combinatorial strategies is of high significance in improving human health. The treatment of cancer patients with autologous chimeric antigen receptor (CAR) T cells is one of the most promising adoptive cellular therapy approaches (86). Recently, the use of CAR T cells in the treatment of chronic lymphocytic leukemia showed that CD19 CAR T cells had an enriched memory gene signature in patients who responded to therapy compared with T cells from nonresponders, who had up-regulated expression of genes involved in effector differentiation, glycolysis, apoptosis, and exhaustion (87). This highlights the significance of promoting memory cell differentiation and survival for enhanced immunotherapy. Thus, using CRISPR/Cas9 to delete Spry1/2 in CAR T cells could be considered in supplementing novel immunotherapies for enhancing antitumor immunity by promoting memory T cell programming in the effectors. The concept of deleting Spry1/2 in CAR T cells to enhance antitumor immunity is also reinforced by a study in which Spry1-deficient

T cells were more proficient than WT T cells at eliminating EL-4 lymphoma and solid B16 tumor cells in mice (30). It remains to be determined whether deleting both *Spry1* and *Spry2* in $CD8^+$ T cells would result in even more efficient antitumor effects.

The formation of larger numbers of functionally superior antigen-specific memory T cells that have enhanced survival is also important in the context of overcoming the immune inhibitory microenvironment of tumors (88–91). For example, under hypoxic conditions in the tumor microenvironment, tumor cells have an enhanced capacity for glucose uptake (92), thus considerably reducing the glucose concentration available to infiltrating effector T cells (93), which depend highly on glycolysis for their effector function (60, 94). In contrast, memory T cells depend on catabolic metabolism marked by enhanced fatty acid oxidation and oxidative phosphorylation (61–63, 95) and thus can better survive the tumor microenvironment while enforcing immunosurveillance (15, 96). Therefore, the development of novel approaches, such as deleting Spry1/2, to boost the number and function of memory T cells has potential for altering T cell metabolism and thus enhancing their antitumor effects.

Materials and Methods

Mice. To generate Spry1/2-floxed mice, we isolated mouse genomic DNA of the *Spry1* and *Spry2* genes from BAC libraries. The Cre-loxP system was used to delete exon 2 of each gene, encompassing the entire protein-coding region. The target regions of *Spry1* and *Spry2* were cloned into the pEasy Flox vector (97). The linearized vectors were electroporated into ES cells (TC1 for *Spry1* and Bruce4 C57BL/6 ES cells for *Spry2*). Drug-resistant ES cell clones were screened for homologous recombination. To obtain chimeric mice, correctly targeted ES clones were injected into BALB/c blastocysts, which were then implanted in CD1 pseudopregnant foster mothers. Chimeric mice were bred to C57BL/6 mice, and the F1 generation was screened for germline transmission of the mutated allele. Mice bearing targeted *Spry1* or *Spry2* allele were screened by PCR. Floxed mice were backcrossed to C57BL/6NCr for 10 generations before intercrossing to create the $Spry1^{flx/flx}Spry2^{flx/flx}$ ($Spry1/2^{flx/flx}$) animals. $Spry1/2^{flx/flx}$ animals were further crossed to CD8Cre (expressed in peripheral T cells) (35) with transgenic expression of either OVA-specific (OT-I) or LCMV gp33-specific (P14) TCRs to generate Spry1/2 DKO T cells. These animals were crossed to the $Rag1^{-/-}$ ($R^{-/-}$) background to eliminate any self-reactivity. Littermate OTI or P14 $Spry1^{flx/flx}$ $Spry2^{flx/flx}$ $CD8Cre^+$ $Rag1^{-/-}$ CD45.1.1 (DKO) or $Spry1^{+/+}$ $Spry2^{+/+}$ $CD8Cre^+$ $Rag1^{-/-}$ CD45.1.2 (WT) were used in the experiments described here.

Mice expressing membrane-bound Ova under the control of the transgenic RIP-mOVA on the C57BL/6 background (36) were crossed to C57BL/6NCr $CD45.2.2^+$ WT mice (National Cancer Institute) and were maintained by crossing to C57BL/6NJ mice (The Jackson Laboratory). Mice were housed and bred in the Gladstone Institutes animal facility. Age- and sex-matched male and female donor and recipient mice (8–20 wk old) were used throughout our studies, and all animal experiments were conducted in accordance with guidelines set by the Institutional Animal Care and Use Committee of the University of California, San Francisco.

Isolation of Immune Cells. Spleens, Med LNs, and peripheral (p)LNs (inguinal, axillary, brachial, and cervical) were homogenized using buffered saline solution, and red blood cells were lysed with ACK lysis buffer (0.15 M NH_4Cl, 10 mM $KHCO_3$, 0.5 mM EDTA). Lungs were isolated and digested as previously described (98). Briefly, the lungs were digested in an enzyme mixture of 6 mL of RPMI-1640 containing collagenase (0.5 mg/mL) (Worthington) and DNase I (0.5 mg/mL) (Sigma-Aldrich) for 45 min at 37 °C. The digested lung tissue was then homogenized, and red blood cells were lysed with ACK lysis buffer. Lymphocytes were further enriched using 27.5% OptiPrep density gradient medium (Sigma-Aldrich).

Flow Cytometry. Cell counts for prepared single-cell suspensions were determined as previously described (47). After blocking Fc receptors with anti-$CD16^+CD32$, 1×10^6 cells from single-cell suspensions were incubated with a mixture of fluorescence-conjugated anti-mouse antibodies for 30 min at 4 °C. Stained cells were washed twice, acquired with an LSR II flow cytometer using FACSDiva software (BD), and analyzed using FlowJo software version 10.2 (TreeStar). The following mAbs (purchased from Thermo Fisher Scientific, BD, or BioLegend) were used: anti-CD8α (SK1), anti-CD45.1 (A20), anti-TCRβ (H57-597), anti-CD69 (H1.2F3), anti-CD27 (LG.3A10), anti-CD45.2 (104), anti-CD45.1 (A20), anti-KLRG1 (2F1), anti-CD127 (SB 199), anti-CD43 (1B11), anti-CD107 (1D4B), anti–IFN-γ (XMG1.2), anti-granzyme B (GB11), anti–TNF-α (MP6-XT22), anti–T-bet (ebio4B10), anti–Ki-67 (B56), anti-S6 (pS235/pS236: N7-548), and anti-4EBP1 (pT36/pT45: M31-16). Anti-$CD16^+CD32$ (2.4G2) antibodies were from the University of California, San Francisco Monoclonal Antibody Core. Antibodies from Cell Signaling, Technology were anti-pAkt (T308:D25E6) and anti–p-FoxO1 (T24)/FoxO3a (T32). For all signaling experiments, cells were first rested in vitro at 37 °C for 2–4 h to ensure that all existing signals returned to background levels before restimulation with 0.1 μM gp33 peptide (GenScript) as previously described (99). Phosphorylated molecules were detected via paraformaldehyde fixation and methanol permeabilization. For detection of p-FoxO1/3a, secondary AF647-conjugated anti-rabbit antibodies were used (Jackson ImmunoResearch Laboratories).

In Vitro Peptide Stimulation and Intracellular Cytokine Staining. Lymphocytes were incubated at 37 °C for 5 h with 1 μM gp33 peptide (GenScript) along with anti-CD107a, and GolgiPlug (BD) was added during the last 4 h of restimulation. This was followed by surface and intracellular staining for cytokine production. The Foxp3 Fixation/Permeabilization Concentrate and Diluent Kit (Thermo Fisher Scientific) was used for intracellular staining.

Glucose Uptake. Glucose uptake was measured with 2-NBDG [2-(*N*-(7-nitrobenz-2-oxa-1,3-diazol-4-yl)amino)-2-deoxyglucose] (Thermo Fisher Scientific). Freshly isolated cells were resuspended in RPMI-1640 medium (Corning) in the presence of 100 μM 2-NBDG and were cultured for 10 min at 37 °C.

Blood and Urine Glucose Measurements. RIP-mOVA transgenic C57BL/6 mice and their WT littermates were injected i.v. with 1×10^6 of either DKO or WT purified OT-I T cells. These mice were subsequently monitored intermittently for a period of 3 wk for blood and urine hyperglycemia. Diabetes was monitored every 2 d after OT-I T cell transfer using a Contour Glucometer (Bayer) and Diastix reagent strips (Bayer) for blood and urine glucose analysis, respectively. Animals that had blood or urine glucose values of >250 mg/dL on two consecutive occasions were counted as diabetic and were killed as described in ref. 100.

Adoptive P14 T Cell Transfer and Infections. For generation of effector and memory P14 $CD8^+$ T cells, naive DKO CD45.1.1 P14 T cells and WT CD45.1.2 P14 T cells were enriched by magnetic bead sorting (STEMCELL Technologies) and were mixed at a 1:1 ratio. Then WT and DKO P14 T cells (2×10^4 cells each) were adoptively cotransferred into CD45.2.2 WT hosts via retroorbital injection. Chimeric animals were infected 24 h later with 2×10^5 pfu $LCMV_{ARM}$ i.p. For priming experiments, P14 T cells were labeled with 0.25 μM CFSE (Thermo Fisher Scientific) at 37 °C for 10 min, and WT and DKO P14 T cells (2.5×10^5 of each) were cotransferred into WT hosts via retroorbital injection. For memory recall, chimeric animals that were immunized i.p. with $LCMV_{ARM}$ were rechallenged 50 d later with 8×10^5 pfu $LCMV_{ARM}$ i.n., and recall responses of memory P14 T cells were measured 2 d later. For i.rec. infections, mice were infected as previously described (47).

***L. monocytogenes* Infection and Determination of Cfus.** Memory P14 T cells from chimeric animals immunized i.p. with $LCMV_{ARM}$ were purified by cell sorting, and 3×10^4 memory P14 T cells of either WT or DKO origin were transferred independently into naive B6 recipients. Mice receiving memory P14 T cells and naive control mice were infected 24 h later with 2×10^5 cfu of virulent *L. monocytogenes* expressing gp33. Two days later, spleen samples were obtained, and bacterial content was analyzed. Spleens were isolated, weighed, placed in 1% FBS in PBS, and homogenized. Single-cell suspensions were made from the spleens of recipient mice in PBS containing 0.5% Triton X-100. Serial dilutions of the supernatants were inoculated on brain-heart-infusion (BHI) agar plates and were incubated for 24 h at 37 °C. Bacterial colonies were enumerated, and cfu were normalized per gram of spleen plated.

RNA Isolation and Quantitative Real-Time PCR. RNA was isolated with TRIzol reagent according to the manufacturer's instructions (Thermo Fisher Scientific). One to five micrograms of RNA was reverse transcribed into cDNA with a Maxima First Strand cDNA Synthesis Kit with dsDNase (Thermo Fisher Scientific). Real-time PCR was performed using 2× SensiFAST probe Hi-Rox mix (Bioline) with gene-specific primers and was run on an ABI Prism 7900 sequence detector with the ΔCt method from SDS 2.4 software (Applied Biosystems). The relative expression of genes was calculated with the formula $2^{-\Delta Ct}$, where ΔCt represents the Ct target gene − Ct endogenous control gene. *Gapdh* was used as the endogenous control housekeeping gene. Viral copies per microgram of RNA were calculated

from a standard curve obtained using serial 10-fold dilutions of LCMV plasmid (101).

For genotyping, the following primers were used:

Spry1: F: acacctcgttcagacagcctcc; R: acactctggggctgaagcagga

Spry2: F: tgttctcctacctcagccac; R: aagacttcccgttctccaccc

For mRNA expression, the following primers were used:

Spry1: F: acctggcaagatcaggatttca; R: tcaccactagcgaagtgtgg

Spry2: F: cagagtttggaaagaaggaaaaagt; R: cacatctgaactccgtgatcg

GAPDH: F: tgtgtccgtcgtggatctga; R: cctgcttcaccaccttcttga

LCMV: F: cattcacctggactttgtcagactc; R: gcaactgctgtgttcccgaaac

Statistical Analyses. All statistical analyses were performed using parametric paired *t* tests or unpaired Mann–Whitney *U* tests, where appropriate. *P* values were also calculated using a log-rank test (diabetes induction experiments). These tests were performed using GraphPad Prism software version 7.0. We considered $P < 0.05$ as statistically significant; $*P < 0.05$, $**P < 0.009$, and $***P < 0.0005$.

ACKNOWLEDGMENTS. We thank J. Luong, F. Wu, and I. Lew for maintaining the mouse colonies; M. Trapecar and S. T. Moss for technical assistance; and C. Palmer (Burnet Institute), L. L. Lanier [University of California, San Francisco (UCSF)], A. Weiss (UCSF), and R. Rutishauser (UCSF) for critical reading of the manuscript. This work was supported by NIH Grants DP2 AI112244 (to S.S.) and NIH UCSF-Gladstone Institute of Virology and Immunology Center for AIDS Research Grant P30-AI027763 (to H.M.S.). This publication was made possible with help from the NIH program Grants P30 AI027763 and S10 RR028962 and the James B. Pendleton Charitable Trust supporting the Gladstone Institutes' flow cytometry core. The Gladstone Institutes' animal care facility received support from National Center for Research Resources Grant RR18928.

1. Lim WA, June CH (2017) The principles of engineering immune cells to treat cancer. *Cell* 168:724–740.
2. Chen DS, Mellman I (2017) Elements of cancer immunity and the cancer-immune set point. *Nature* 541:321–330.
3. Wherry EJ, Kurachi M (2015) Molecular and cellular insights into T cell exhaustion. *Nat Rev Immunol* 15:486–499.
4. Ahmed R, Gray D (1996) Immunological memory and protective immunity: Understanding their relation. *Science* 272:54–60.
5. Badovinac VP, Messingham KA, Hamilton SE, Harty JT (2003) Regulation of CD8+ T cells undergoing primary and secondary responses to infection in the same host. *J Immunol* 170:4933–4942.
6. Kaech SM, Ahmed R (2001) Memory CD8+ T cell differentiation: Initial antigen encounter triggers a developmental program in naïve cells. *Nat Immunol* 2:415–422.
7. Schmidt NW, et al. (2008) Memory CD8 T cell responses exceeding a large but definable threshold provide long-term immunity to malaria. *Proc Natl Acad Sci USA* 105:14017–14022.
8. Jameson SC, Masopust D (2018) Understanding subset diversity in T cell memory. *Immunity* 48:214–226.
9. Kumar BV, Connors TJ, Farber DL (2018) Human T cell development, localization, and function throughout life. *Immunity* 48:202–213.
10. Mueller SN, Mackay LK (2016) Tissue-resident memory T cells: Local specialists in immune defence. *Nat Rev Immunol* 16:79–89.
11. Araki K, et al. (2009) mTOR regulates memory CD8 T-cell differentiation. *Nature* 460: 108–112.
12. Pearce EL, et al. (2009) Enhancing CD8 T-cell memory by modulating fatty acid metabolism. *Nature* 460:103–107.
13. Kim MV, Ouyang W, Liao W, Zhang MQ, Li MO (2013) The transcription factor Foxo1 controls central-memory CD8+ T cell responses to infection. *Immunity* 39: 286–297.
14. Rao RR, Li Q, Odunsi K, Shrikant PA (2010) The mTOR kinase determines effector versus memory CD8+ T cell fate by regulating the expression of transcription factors T-bet and Eomesodermin. *Immunity* 32:67–78.
15. Sukumar M, et al. (2013) Inhibiting glycolytic metabolism enhances CD8+ T cell memory and antitumor function. *J Clin Invest* 123:4479–4488.
16. Pollizzi KN, et al. (2015) mTORC1 and mTORC2 selectively regulate $CD8^+$ T cell differentiation. *J Clin Invest* 125:2090–2108.
17. Jameson SC, Masopust D (2009) Diversity in T cell memory: An embarrassment of riches. *Immunity* 31:859–871.
18. Chang JT, Wherry EJ, Goldrath AW (2014) Molecular regulation of effector and memory T cell differentiation. *Nat Immunol* 15:1104–1115.
19. Kaech SM, Cui W (2012) Transcriptional control of effector and memory CD8+ T cell differentiation. *Nat Rev Immunol* 12:749–761.
20. Kamphorst AO, Araki K, Ahmed R (2015) Beyond adjuvants: Immunomodulation strategies to enhance T cell immunity. *Vaccine* 33:B21–B28.
21. Sharpe AH, Pauken KE (2018) The diverse functions of the PD1 inhibitory pathway. *Nat Rev Immunol* 18:153–167.
22. Wei SC, et al. (2017) Distinct cellular mechanisms underlie anti-CTLA-4 and anti-PD-1 checkpoint blockade. *Cell* 170:1120–1133.e1117.
23. Sharma P, Allison JP (2015) The future of immune checkpoint therapy. *Science* 348: 56–61.
24. Choi H, Cho SY, Schwartz RH, Choi K (2006) Dual effects of Sprouty1 on TCR signaling depending on the differentiation state of the T cell. *J Immunol* 176:6034–6045.
25. Hacohen N, Kramer S, Sutherland D, Hiromi Y, Krasnow MA (1998) Sprouty encodes a novel antagonist of FGF signaling that patterns apical branching of the Drosophila airways. *Cell* 92:253–263.
26. Gross I, Bassit B, Benezra M, Licht JD (2001) Mammalian sprouty proteins inhibit cell growth and differentiation by preventing ras activation. *J Biol Chem* 276: 46460–46468.
27. Hanafusa H, Torii S, Yasunaga T, Nishida E (2002) Sprouty1 and Sprouty2 provide a control mechanism for the Ras/MAPK signalling pathway. *Nat Cell Biol* 4:850–858.
28. Lee JS, et al. (2009) Recruitment of Sprouty1 to immune synapse regulates T cell receptor signaling. *J Immunol* 183:7178–7186.
29. Akbulut S, et al. (2010) Sprouty proteins inhibit receptor-mediated activation of phosphatidylinositol-specific phospholipase C. *Mol Biol Cell* 21:3487–3496.
30. Collins S, et al. (2012) Regulation of $CD4^+$ and $CD8^+$ effector responses by Sprouty-1. *PLoS One* 7:e49801.
31. Chiu YL, et al. (2014) Sprouty-2 regulates HIV-specific T cell polyfunctionality. *J Clin Invest* 124:198–208.
32. Dikic I, Giordano S (2003) Negative receptor signalling. *Curr Opin Cell Biol* 15: 128–135.
33. Guy GR, et al. (2003) Sprouty: How does the branch manager work? *J Cell Sci* 116: 3061–3068.
34. Mason JM, Morrison DJ, Basson MA, Licht JD (2006) Sprouty proteins: Multifaceted negative-feedback regulators of receptor tyrosine kinase signaling. *Trends Cell Biol* 16:45–54.
35. Maekawa Y, et al. (2008) Notch2 integrates signaling by the transcription factors RBP-J and CREB1 to promote T cell cytotoxicity. *Nat Immunol* 9:1140–1147.
36. Kurts C, et al. (1996) Constitutive class I-restricted exogenous presentation of self antigens in vivo. *J Exp Med* 184:923–930.
37. Kurts C, et al. (1997) CD4+ T cell help impairs CD8+ T cell deletion induced by cross-presentation of self-antigens and favors autoimmunity. *J Exp Med* 186:2057–2062.
38. Olson MR, McDermott DS, Varga SM (2012) The initial draining lymph node primes the bulk of the CD8 T cell response and influences memory T cell trafficking after a systemic viral infection. *PLoS Pathog* 8:e1003054.
39. Matsumoto M, et al. (2007) CD43 collaborates with P-selectin glycoprotein ligand-1 to mediate E-selectin-dependent T cell migration into inflamed skin. *J Immunol* 178:2499–2506.
40. Hand TW, Kaech SM (2009) Intrinsic and extrinsic control of effector T cell survival and memory T cell development. *Immunol Res* 45:46–61.
41. Marrack P, Kappler J (2004) Control of T cell viability. *Annu Rev Immunol* 22:765–787.
42. Kaech SM, et al. (2003) Selective expression of the interleukin 7 receptor identifies effector CD8 T cells that give rise to long-lived memory cells. *Nat Immunol* 4: 1191–1198.
43. Joshi NS, et al. (2007) Inflammation directs memory precursor and short-lived effector CD8(+) T cell fates via the graded expression of T-bet transcription factor. *Immunity* 27:281–295.
44. Sarkar S, et al. (2008) Functional and genomic profiling of effector CD8 T cell subsets with distinct memory fates. *J Exp Med* 205:625–640.
45. Olson JA, McDonald-Hyman C, Jameson SC, Hamilton SE (2013) Effector-like $CD8^+$ T cells in the memory population mediate potent protective immunity. *Immunity* 38: 1250–1260.
46. Gerlach C, et al. (2016) The chemokine receptor CX3CR1 defines three antigen-experienced CD8 T cell subsets with distinct roles in immune surveillance and homeostasis. *Immunity* 45:1270–1284.
47. Trapecar M, Khan S, Cohn BL, Wu F, Sanjabi S (2018) B cells are the predominant mediators of early systemic viral dissemination during rectal LCMV infection. *Mucosal Immunol* 11:1158–1167.
48. Khan S, et al. (2016) Dampened antiviral immunity to intravaginal exposure to RNA viral pathogens allows enhanced viral replication. *J Exp Med* 213:2913–2929.
49. Hikono H, et al. (2007) Activation phenotype, rather than central- or effector-memory phenotype, predicts the recall efficacy of memory CD8+ T cells. *J Exp Med* 204:1625–1636.
50. Rao RR, Li Q, Gubbels Bupp MR, Shrikant PA (2012) Transcription factor Foxo1 represses T-bet-mediated effector functions and promotes memory CD8(+) T cell differentiation. *Immunity* 36:374–387.
51. Zhang L, et al. (2016) Mammalian target of rapamycin complex 2 controls CD8 T cell memory differentiation in a Foxo1-dependent manner. *Cell Rep* 14:1206–1217.
52. Rogel A, et al. (2017) Akt signaling is critical for memory $CD8^+$ T-cell development and tumor immune surveillance. *Proc Natl Acad Sci USA* 114:E1178–E1187.
53. Li Q, et al. (2011) A central role for mTOR kinase in homeostatic proliferation induced CD8+ T cell memory and tumor immunity. *Immunity* 34:541–553.
54. Intlekofer AM, et al. (2007) Requirement for T-bet in the aberrant differentiation of unhelped memory CD8+ T cells. *J Exp Med* 204:2015–2021.
55. Banerjee A, et al. (2010) Cutting edge: The transcription factor eomesodermin enables CD8+ T cells to compete for the memory cell niche. *J Immunol* 185:4988–4992.

56. Intlekofer AM, et al. (2005) Effector and memory CD8+ T cell fate coupled by T-bet and eomesodermin. *Nat Immunol* 6:1236–1244.
57. Pollizzi KN, et al. (2016) Asymmetric inheritance of mTORC1 kinase activity during division dictates CD8(+) T cell differentiation. *Nat Immunol* 17:704–711.
58. Alessi DR, et al. (1997) Characterization of a 3-phosphoinositide-dependent protein kinase which phosphorylates and activates protein kinase Balpha. *Curr Biol* 7: 261–269.
59. Sarbassov DD, Guertin DA, Ali SM, Sabatini DM (2005) Phosphorylation and regulation of Akt/PKB by the rictor-mTOR complex. *Science* 307:1098–1101.
60. Shehata HM, et al. (2017) Sugar or fat?-Metabolic requirements for immunity to viral infections. *Front Immunol* 8:1311.
61. van der Windt GJW, et al. (2012) Mitochondrial respiratory capacity is a critical regulator of CD8+ T cell memory development. *Immunity* 36:68–78.
62. van der Windt GJW, et al. (2013) CD8 memory T cells have a bioenergetic advantage that underlies their rapid recall ability. *Proc Natl Acad Sci USA* 110:14336–14341.
63. O'Sullivan D, et al. (2014) Memory CD8(+) T cells use cell-intrinsic lipolysis to support the metabolic programming necessary for development. *Immunity* 41:75–88.
64. Finlay DK, et al. (2012) PDK1 regulation of mTOR and hypoxia-inducible factor 1 integrate metabolism and migration of CD8+ T cells. *J Exp Med* 209:2441–2453.
65. Chan AC, Iwashima M, Turck CW, Weiss A (1992) ZAP-70: A 70 kd protein-tyrosine kinase that associates with the TCR zeta chain. *Cell* 71:649–662.
66. Zhang W, Sloan-Lancaster J, Kitchen J, Trible RP, Samelson LE (1998) LAT: The ZAP-70 tyrosine kinase substrate that links T cell receptor to cellular activation. *Cell* 92: 83–92.
67. Imboden JB, Stobo JD (1985) Transmembrane signalling by the T cell antigen receptor. Perturbation of the T3-antigen receptor complex generates inositol phosphates and releases calcium ions from intracellular stores. *J Exp Med* 161:446–456.
68. Abraham RT, Weiss A (2004) Jurkat T cells and development of the T-cell receptor signalling paradigm. *Nat Rev Immunol* 4:301–308.
69. Tamás P, et al. (2006) Regulation of the energy sensor AMP-activated protein kinase by antigen receptor and Ca2+ in T lymphocytes. *J Exp Med* 203:1665–1670.
70. Inoki K, Zhu T, Guan KL (2003) TSC2 mediates cellular energy response to control cell growth and survival. *Cell* 115:577–590.
71. Kimura N, et al. (2003) A possible linkage between AMP-activated protein kinase (AMPK) and mammalian target of rapamycin (mTOR) signalling pathway. *Genes Cells* 8:65–79.
72. Blagih J, et al. (2015) The energy sensor AMPK regulates T cell metabolic adaptation and effector responses in vivo. *Immunity* 42:41–54.
73. Fong CW, et al. (2003) Tyrosine phosphorylation of Sprouty2 enhances its interaction with c-Cbl and is crucial for its function. *J Biol Chem* 278:33456–33464.
74. Wong ES, Lim J, Low BC, Chen Q, Guy GR (2001) Evidence for direct interaction between sprouty and Cbl. *J Biol Chem* 276:5866–5875.
75. Egan JE, Hall AB, Yatsula BA, Bar-Sagi D (2002) The bimodal regulation of epidermal growth factor signaling by human sprouty proteins. *Proc Natl Acad Sci USA* 99: 6041–6046.
76. Fang D, Liu YC (2001) Proteolysis-independent regulation of PI3K by Cbl-b-mediated ubiquitination in T cells. *Nat Immunol* 2:870–875.
77. Robert C, et al. (2011) Ipilimumab plus dacarbazine for previously untreated metastatic melanoma. *N Engl J Med* 364:2517–2526.
78. Hodi FS, et al. (2010) Improved survival with ipilimumab in patients with metastatic melanoma. *N Engl J Med* 363:711–723.
79. Reichert JM (2012) Marketed therapeutic antibodies compendium. *MAbs* 4:413–415.
80. Ribas A, et al. (2013) Phase III randomized clinical trial comparing tremelimumab with standard-of-care chemotherapy in patients with advanced melanoma. *J Clin Oncol* 31:616–622.
81. Chung KY, et al. (2010) Phase II study of the anti-cytotoxic T-lymphocyte-associated antigen 4 monoclonal antibody, tremelimumab, in patients with refractory metastatic colorectal cancer. *J Clin Oncol* 28:3485–3490.
82. Phan GQ, et al. (2003) Cancer regression and autoimmunity induced by cytotoxic T lymphocyte-associated antigen 4 blockade in patients with metastatic melanoma. *Proc Natl Acad Sci USA* 100:8372–8377.
83. Ribas A, et al. (2005) Antitumor activity in melanoma and anti-self responses in a phase I trial with the anti-cytotoxic T lymphocyte-associated antigen 4 monoclonal antibody CP-675,206. *J Clin Oncol* 23:8968–8977.
84. Beck KE, et al. (2006) Enterocolitis in patients with cancer after antibody blockade of cytotoxic T-lymphocyte-associated antigen 4. *J Clin Oncol* 24:2283–2289.
85. Downey SG, et al. (2007) Prognostic factors related to clinical response in patients with metastatic melanoma treated by CTL-associated antigen-4 blockade. *Clin Cancer Res* 13:6681–6688.
86. Wang X, Rivière I (2016) Clinical manufacturing of CAR T cells: Foundation of a promising therapy. *Mol Ther Oncolytics* 3:16015.
87. Fraietta JA, et al. (2018) Determinants of response and resistance to CD19 chimeric antigen receptor (CAR) T cell therapy of chronic lymphocytic leukemia. *Nat Med* 24: 563–571.
88. Pedicord VA, Montalvo W, Leiner IM, Allison JP (2011) Single dose of anti-CTLA-4 enhances CD8+ T-cell memory formation, function, and maintenance. *Proc Natl Acad Sci USA* 108:266–271.
89. Ribas A, et al. (2016) PD-1 blockade expands intratumoral memory T cells. *Cancer Immunol Res* 4:194–203.
90. Allie SR, Zhang W, Fuse S, Usherwood EJ (2011) Programmed death 1 regulates development of central memory CD8 T cells after acute viral infection. *J Immunol* 186:6280–6286.
91. Bally AP, et al. (2017) Conserved region C functions to regulate PD-1 expression and subsequent CD8 T cell memory. *J Immunol* 198:205–217.
92. Ward PS, Thompson CB (2012) Metabolic reprogramming: A cancer hallmark even warburg did not anticipate. *Cancer Cell* 21:297–308.
93. Ho PC, Kaech SM (2017) Reenergizing T cell anti-tumor immunity by harnessing immunometabolic checkpoints and machineries. *Curr Opin Immunol* 46:38–44.
94. Gubser PM, et al. (2013) Rapid effector function of memory CD8+ T cells requires an immediate-early glycolytic switch. *Nat Immunol* 14:1064–1072.
95. Buck MD, O'Sullivan D, Pearce EL (2015) T cell metabolism drives immunity. *J Exp Med* 212:1345–1360.
96. Crompton JG, et al. (2015) Akt inhibition enhances expansion of potent tumor-specific lymphocytes with memory cell characteristics. *Cancer Res* 75:296–305.
97. Schenten D, et al. (2002) DNA polymerase kappa deficiency does not affect somatic hypermutation in mice. *Eur J Immunol* 32:3152–3160.
98. Sanjabi S, Mosaheb MM, Flavell RA (2009) Opposing effects of TGF-beta and IL-15 cytokines control the number of short-lived effector CD8+ T cells. *Immunity* 31: 131–144.
99. Staron MM, et al. (2014) The transcription factor FoxO1 sustains expression of the inhibitory receptor PD-1 and survival of antiviral CD8(+) T cells during chronic infection. *Immunity* 41:802–814.
100. Ouyang W, Beckett O, Ma Q, Li MO (2010) Transforming growth factor-beta signaling curbs thymic negative selection promoting regulatory T cell development. *Immunity* 32:642–653.
101. McCausland MM, Crotty S (2008) Quantitative PCR technique for detecting lymphocytic choriomeningitis virus in vivo. *J Virol Methods* 147:167–176.